ACCOUNTS
of chemical research

Single-Molecule Electrochemistry: Present Status and Outlook

SERGE G. LEMAY,* SHUO KANG, KLAUS MATHWIG, AND PRADYUMNA S. SINGH

MESA+ Institute for Nanotechnology, University of Twente, PO Box 217, 7500 AE Enschede, The Netherlands

RECEIVED ON JUNE 4, 2012

CONSPECTUS

The development of methods for detecting and manipulating matter at the level of individual macromolecules represents one of the key scientific advancements of recent decades. These techniques allow us to get information that is largely unobtainable otherwise, such as the magnitudes of microscopic forces, mechanistic details of catalytic processes, macromolecular population heterogeneities, and time-resolved, step-by-step observation of complex kinetics. Methods based on optical, mechanical, and ionic-conductance signal transduction are particularly developed. However, there is scope for new approaches that can broaden the range of molecular systems that we can study at this ultimate level of sensitivity and for developing new analytical methods relying on single-molecule detection. Approaches based on purely electrical detection are particularly appealing in the latter context, since they can be easily combined with microelectronics or fluidic devices on a single microchip to create large parallel assays at relatively low cost.

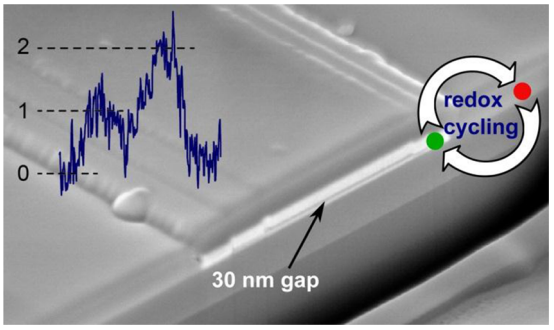

A form of electrical signal transduction that has so far remained relatively underdeveloped at the single-molecule level is the direct detection of the charge transferred in electrochemical processes. The reason for this is simple: only a few electrons are transferred per molecule in a typical faradaic reaction, a heterogeneous charge-transfer reaction that occurs at the electrode's surface. Detecting this tiny amount of charge is impossible using conventional electrochemical instrumentation. A workaround is to use redox cycling, in which the charge transferred is amplified by repeatedly reducing and oxidizing analyte molecules as they randomly diffuse between a pair of electrodes. For this process to be sufficiently efficient, the electrodes must be positioned within less than 100 nm of each other, and the analyte must remain between the electrodes long enough for the measurement to take place. Early efforts focused on tip-based nanoelectrodes, descended from scanning electrochemical microscopy, to create suitable geometries. However, it has been challenging to apply these technologies broadly.

In this Account, we describe our alternative approach based on electrodes embedded in microfabricated nanochannels, so-called nanogap transducers. Microfabrication techniques grant a high level of reproducibility and control over the geometry of the devices, permitting systematic development and characterization. We have employed these devices to demonstrate single-molecule sensitivity. This method shows good agreement with theoretical analysis based on the Brownian motion of discrete molecules, but only once the finite time resolution of the experimental apparatus is taken into account. These results highlight both the random nature of single-molecule signals and the complications that it can introduce in data interpretation. We conclude this Account with a discussion on how scientists can overcome this limitation in the future to create a new experimental platform that can be generally useful for both fundamental studies and analytical applications.

Introduction

Experimental methods capable of detecting and manipulating individual molecules are evocative of Maxwell's Demon, the hypothetical imp introduced by 19th century physicist James Clerk Maxwell in his writings on the Second Law of Thermodynamics.[1] That we can now realize what was originally considered a pure thought experiment bears testimony to the advances in experimental science since Maxwell's time. Indeed, the last two decades have seen an explosion in methods capable of addressing individual (macro)molecules. While rapid development continues, the main techniques constituting this so-called

Published on the Web 12/27/2012 www.pubs.acs.org/accounts
10.1021/ar300169d

"single-molecule toolkit"[2,3] have now become relatively mature, with optical[4] and mechanical[5] signal transduction dominating. It is however fair to wonder whether the toolkit can be further extended, for example, to the realm of purely electrochemical approaches.

Why should one be interested in performing electrochemistry near or at the single-molecule limit, apart from the satisfaction of reaching one of the fundamental limits imposed by the inherent graininess of matter? There are, in our opinion, three main motivations. First, measurements on the molecular scale allow revisiting the fundamentals of electron-transfer reactions in regimes where they have not been tested before, thus probing the limits of long-established assumptions.[6] This addresses all aspects of electrochemistry, including double-layer structure, mass transport, heterogeneous kinetics, and the statistical nature of processes on this scale. Second, one can envision new types of electrochemical assays on mesoscale systems such as individual living cells, in which the absolute number of target molecules is inherently limited to a few copies, or that exploit single-molecule fingerprinting for increasing the selectivity of faradaic detection. Third, new techniques are enablers of fundamental experiments on nanoscale systems, providing a new window on population heterogeneities and the microscopic dynamics of systems ranging from catalytic nanoparticles to single enzymes. A dramatic example of the potential of such developments is provided by methods for measuring the elastic response of nucleic acids: originally perceived by many as a narrow exercise in polymer physics, they have instead allowed attacking problems ranging from nonequilibrium statistical mechanics[7] to the microscopic workings of DNA-binding proteins.[8,9]

Redox Cycling

The direct detection of the few electrons transferred in a typical faradaic process, while possible at cryogenic temperatures, represents a nearly insurmountable challenge at electrodes in contact with room-temperature liquids. This is in contrast to monitoring a molecule's redox state using fluorescence[13−15] or surface-enhanced Raman spectroscopy,[16] as well as alternative electrical methods such as nanoscale pores,[17−20] scanning probe microscopy,[6,21] break junctions,[22−24] and catalytic amplification.[25] Detection of individual molecules through electron-transfer reactions thus requires a means of increasing the number of electrons involved. This charge amplification can be achieved by redox cycling, which relies on a thin-layer-cell geometry

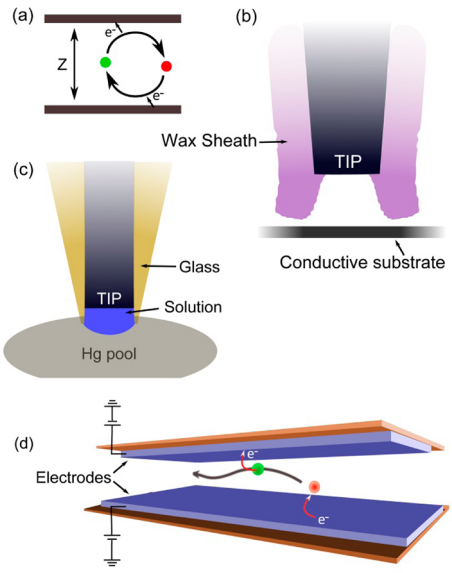

FIGURE 1. Electrochemical single-molecule detection. (a) Basic concept of redox cycling. (b) Nanoelectrode encased in wax and positioned near a metallic surface.[10] (c) Recessed glass-encased nanoelectrode immersed in mercury.[11] (d) Lithographically fabricated nanogap device.[12]

consisting of two parallel electrodes; the electrodes are biased such that target molecules undergo repeated alternating reduction and oxidation, as illustrated in Figure 1a. Each redox molecule thus shuttles thousands or even millions of electrons per second between the electrodes, generating a current that is large enough to be detected. This approach is in principle applicable for all redox species that are chemically reversible, that is, whose reduced and oxidized forms are both stable over the time scale of the measurement. First introduced by Reilley and coworkers,[26,27] redox cycling was harnessed by Fan and Bard in their pioneering single-molecule experiment[10] and has provided the basis for all attempts since.[11,12]

Theoretical Background

Measurements dealing with single or few molecules inherently include a component of randomness. In particular, underlying Fick's laws, deterministic equations that describe average diffusive mass transport, is the purely random Brownian motion of individual particles.[28,29] This randomness does not mean that it is impossible to extract quantitative information from single-molecule data, however. Encoded in stochastic signals is a wealth of information, albeit uncovering it requires a change of perspective from how we look at more familiar "macroscopic" data. This opportunity to validate single-molecule experiments has so far not been exploited to the fullest in the field of electrochemistry.

Consider a macroscopic volume of electrolyte containing redox molecules at concentration C. A much smaller subvolume V is then sampled. The average number of molecules, $\langle N\rangle$ in this subvolume is simply given by $\langle N\rangle = N_A VC$, where N_A is Avogadro's number. Any particular sampling may however capture fewer or more molecules due to chance. The probability $P(N)$ of finding exactly N molecules in the subvolume is given by the Poisson distribution,[30]

$$P(N) = \frac{\langle N\rangle^N \, e^{-\langle N\rangle}}{N!} \tag{1}$$

This distribution has a standard deviation of $\langle N\rangle^{1/2}$, so the relative size of the fluctuations is negligible compared with $\langle N\rangle$ when $\langle N\rangle$ is large, a manifestation of the law of large numbers. For $\langle N\rangle$ of order unity, on the other hand, the size of the fluctuations is comparable to $\langle N\rangle$ itself; the system is then manifestly stochastic in nature.

Suppose that we are instead interested in a small volume in diffusive equilibrium with a larger reservoir, such that molecules can freely diffuse in and out of this small volume. In this case, eq 1 still gives the probability of finding exactly N particles in the small volume at a given time, but N can now fluctuate in time: $N = N(t)$. These fluctuations are not deviations from equilibrium: on the contrary, they are an intrinsic feature of open systems with a well-defined chemical potential. The process, while random, does not follow arbitrary rules: given the geometry, it is relatively straightforward to predict[31] the power spectrum of the fluctuations in $N(t)$ (or, equivalently, its Fourier transform, the autocorrelation function[32,33]). This provides a unique opportunity to verify whether experimentally observed stochastic signals can be attributed to single-molecule fluctuations.

In a typical nanogap electrochemistry experiment, the volume of liquid between the two electrodes plays the role of small volume V. Each redox molecule inside this active region shuttles electrons between the two electrodes as it undergoes Brownian motion. The shuttling is itself a stochastic process: the time taken for the redox molecule to travel from one electrode to the other and back again differs with each cycle, so electrons are transferred at random intervals. In practice, however, this particular source of randomness can often be ignored because the shuttling process is too fast to be resolved experimentally (<1 μs for a 10 nm electrode spacing).[34] Each molecule therefore contributes a fixed current, i_0, yielding for the total current, $I(t)$

$$I(t) = i_0 N(t) \tag{2}$$

What is the magnitude of the change in current when a single molecule enters or leaves the detection volume? For the well-known case of unhindered Brownian motion (corresponding to a high supporting electrolyte concentration) and large overpotentials at both oxidizing and reducing electrodes, it is easily shown by solving the one-dimensional diffusion equation that i_0 is given by[10]

$$i_{0,\,\mathrm{ideal}} = \frac{enD}{z^2} \tag{3}$$

where $-e$ is the charge of the electron, n is the number of electrons transferred, D is the diffusion coefficient of the redox species, and z is the distance between the electrodes. That this current is proportional to $1/z^2$ highlights the key experimental requirement for maximum sensitivity: the electrodes must be brought as close to each other as possible. Experimentally, a readily accessible current scale is ~1 pA, while currents below 10 fA are difficult to measure; combined with a typical diffusion coefficient, $D \approx 1 \times 10^{-9}$ m^2/s, eq 3 indicates that z should be in the range 10−100 nm. Because the term "nanometer-scale thin-layer cell" is somewhat cumbersome, we use the short-hand "nanogap device" below.

Importantly, the value of i_0 usually differs from $i_{0,\mathrm{ideal}}$. Some factors responsible include electron-transfer kinetics[35,36] (lowering i_0) and migration effects at moderate supporting electrolyte concentrations[37] (increasing or lowering i_0). Transient adsorption of the redox molecules to the electrodes also causes i_0 to decrease since molecules do not shuttle electrons while adsorbed. This is a particularly subtle point since adsorption cannot be diagnosed from the value of the average diffusion-limited current, which is given by $I = neDN_A CA/z$, with A being the area of the electrodes, whether or not adsorption takes place.[31]

Providing unequivocal proof of single-molecule detection thus remains a challenging proposition. Equation 3 only indicates the expected current level under the assumption of an ideal, purely diffusive system without adsorption: coupled with the fact that single-molecule experiments are usually performed in the presence of unwanted background currents, this renders problematic any inference based solely on the absolute current level. Unambiguous demonstration of single-molecule sensitivity therefore calls for additional, complementary arguments. Fortunately, eq 2, while succinct,

makes a powerful prediction: insofar as the time-dependent variations in the number of molecules in the nanogap can be (statistically) predicted, experiments can be confronted with theory via amperometric measurements. Thus, while "noise" is usually considered an unwanted hindrance, here it provides a route for validating single-molecule sensitivity.

Experiments

A survey of the literature on single-molecule electrochemistry measurements is remarkably brief,[10−12,30,32] a sign of the formidable experimental challenge still posed by this problem.

The first report of single-molecule detection by electrochemical means was published in 1995.[10] Fan and Bard created a nanogap by approaching a Pt−Ir tip to within ∼10 nm of a conductive substrate using a scanning electrochemical microscope (SECM). An insulating wax shroud provided confinement in the lateral direction (diameter = tens of nanometers), as illustrated in Figure 1b. At concentrations where $\langle N \rangle$ was of order unity (based on the estimated volume of the cavity), large relative fluctuations were observed in the faradaic current with a ∼10 s duration. Some of these fluctuations had a step-like character with a step height consistent with pure diffusion, as per eq 3, and these features were attributed to fluctuations in $N(t)$ inside the nanogap. Because diffusive mass transport in such small systems takes place on the submicrosecond time scale, orders of magnitude faster than the observed fluctuations, the authors postulated that the fluctuations were instead due to imperfections in the wax shroud such as cracks or other trap sites for redox molecules. Unfortunately, in the absence of sufficiently extensive data or independent information about the trapping dynamics, quantitative comparison to theoretical predictions such as eq 1 could not be performed.[30,32]

More than a decade elapsed before Sun and Mirkin reported a new independent effort at single-molecule detection.[11] The experiment employed a disk-like recessed Pt nanoelectrode shrouded in glass. As illustrated in Figure 1c, solution was trapped between the electrode and a Hg bath, creating a nanogap geometry. The observed faradaic current level, while quite reproducible between different experiments at high redox species concentrations, exhibited large variations at concentrations such that $\langle N \rangle \approx 1$. The rough magnitude of the fluctuations was consistent with eq 3, and the variations were attributed to different numbers of redox molecules N being trapped inside the nanogap. Neither time-dependent jumps as observed by Fan and Bard nor signatures of finite redox molecule lifetime were reported; the extent of the data also did not allow a quantitative comparison to eq 1. Interestingly, interpretation of the measurements necessitated invoking double-layer effects, highlighting the influence of the high surface-to-volume ratio inherent in nanogaps.

Our group's efforts in single-molecule electrochemistry[12] were originally stimulated by the work of Fan and Bard,[10,32] and our early (unpublished) experiments were also based on tip-based nanoelectrodes. We soon abandoned this approach, however, for three interconnected reasons. First, reproducibly fabricating nanoelectrodes proved difficult and labor-intensive. Second, the shape and size of nanoscale electrodes remain difficult to characterize (despite recent progress[38]), and electrochemistry is often the main characterization tool available.[39,40] Since we aimed at exploring new electrochemical regimes, where conventional results cannot *a priori* be assumed to hold, we favored approaches where independent characterization of the geometry is more readily feasible. Third, since we ultimately aimed to use single-molecule electrochemistry as a platform for a broad spectrum of further fundamental and applied research, we favored approaches that maximize flexibility and reproducibility.

These considerations led us to pursue a completely different strategy based on lithographic microfabrication techniques. The basic geometry of our devices is illustrated in Figure 1d. Microfabrication offers several advantages, which we believe are critical for further development and broader applicability of single-molecule electrochemistry: (1) During fabrication, multiple devices are fabricated in parallel; for example, hundreds of monolithic devices can be fabricated simultaneously on a single wafer. These devices are nominally identical, allowing for systematic experimental studies. As a longer-term prospect, $\sim 10^5$ devices could in principle be fit in a square centimeter if the readout electronics were integrated on the same chip.[41] (2) Independent characterization of the devices is greatly facilitated. In particular, parallel fabrication allows sacrificing devices for characterization while other, pristine devices are retained for measurements. Test structures can also be fabricated simultaneously on the same chip. (3) The resulting knowledge about device geometry greatly reduces the number of unknowns when modeling the devices theoretically. (4) Because standard, well-proven processes are employed, the vast expertise that exists in the field of lithography-based fabrication can be harnessed. Systematic, iterative design can be employed to improve device reliability

and performance. (5) Microfabrication yields great flexibility. For example, rather than being confined to a single geometry dictated by the fabrication method, nanogap devices can be made in a variety of shapes,[42] arrays of transducers can be created,[43] and the devices can be integrated with micro/nanofluidic components such as channels, valves, and pumps.[33,43−45]

Lithographically Fabricated Nanogaps

Lithography-based microfabrication techniques are based on the successive deposition and patterning of films of conductive and insulating materials that allow construction of complex three-dimensional structures;[44] detailed protocols for fabricating nanogap devices have been described elsewhere.[12,35,44,45] This approach grants excellent control over the most important parameter in redox cycling, namely, the distance between the electrodes, *z*, using a so-called sacrificial layer technique. A three-layer stack is first constructed that consists of the bottom electrode material, a sacrificial layer (amorphous silicon[46] or chromium[35]), and the top electrode. Once the rest of the device is completed, the sacrificial layer is etched away and replaced with solution, thus creating the nanogap geometry. The thickness of the sacrificial layer can be carefully controlled and characterized, thereby providing an independent handle on the electrode spacing, *z*. In practice, the main factor limiting the smallest achievable *z* is the risk of the electrodes being short-circuited, especially near the edges of the electrodes (where some roughness caused during patterning is difficult to avoid). At the time of writing, spacings of ∼50 nm can be routinely fabricated,[35,47] devices with $z = 30$ nm have been demonstrated,[12] and efforts are underway to further downscale to $z < 20$ nm. Figure 2 illustrates a particular geometry.

Lithographically fabricated nanogap devices also have drawbacks compared with tip-based electrodes: (1) Production requires access to microfabrication facilities, whereas tip-based electrodes require only a comparatively modest investment. The devices can however be stored for years, provided that etching of the sacrificial layer (by applying a drop of etchant solution) occurs immediately prior to use. One can thus envision devices being microfabricated in bulk and distributed as consumables, mitigating this issue. (2) The geometry of nanogap devices is fixed at the time of fabrication; one cannot vary *z* in the same way as in SECM. (3) The smallest electrode spacing fabricated so far remains larger than has been reported for nanoelectrodes.[10,11] (4) The lateral dimensions of microfabricated nanogaps is in the micrometer range, resulting in larger volumes than

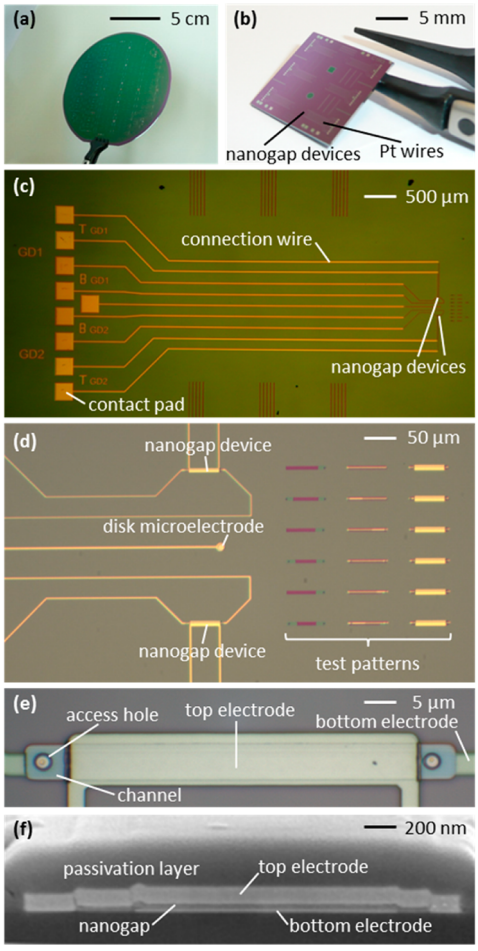

FIGURE 2. Lithography-based nanogap devices. (a) Silicon wafer with devices. (b) Silicon die cut from a wafer with 12 discrete nanogap transducers; the gray features are Pt wires. (c) Optical image showing two devices and associated wires. Contact to external instrumentation is made via the square contact pads on the left. (d) Zoomed-in view of the two devices. Also visible are an integrated microelectrode and test patterns for monitoring the fabrication process. (e) Details of a single nanogap device.[42] (f) Scanning electron micrograph of the cross-section of a device ($z = 30$ nm). Panel f reproduced from ref 12. Copyright 2011 American Chemical Society.

for nanoelectrodes (femtoliters vs zeptoliters); reaching the single-molecule limit thus requires lower analyte concentrations.

In our measurements, the current at both electrodes is measured independently using a three-electrode configuration (two working electrodes and an external reference, which also serves as counter electrode). Figure 3a shows amperometry data in acetonitrile with 0.1 M tetrabutylammonium hexafluorophosphate ($TBAPF_6$) as supporting electrolyte under redox cycling conditions but in the absence of intentionally added redox species. The current through both electrodes exhibits noise that originates primarily from the measurement circuit. Figure 3b shows a corresponding

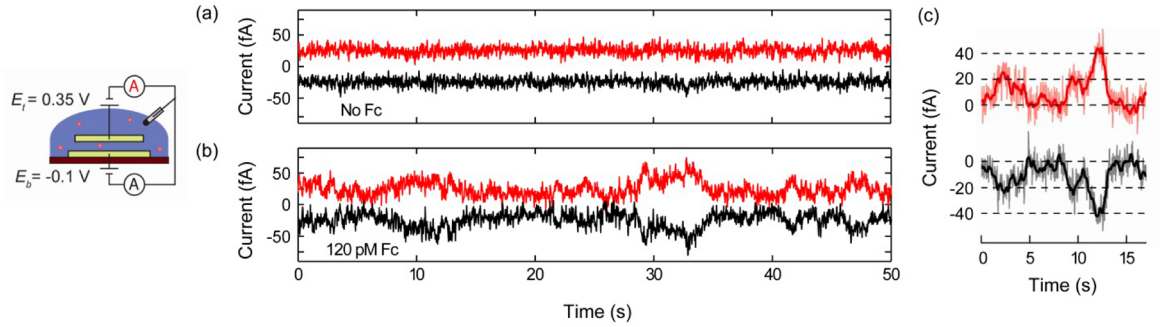

FIGURE 3. Amperometric detection of single molecules. (a) Measured current vs time at the top (red) and bottom (black) electrodes in the absence of redox-active molecules. (b) Corresponding measurement in the presence of 120 pM Fc ($\langle N \rangle = 0.4$). (c) Zoom-in of a particularly long event exhibiting current plateaus corresponding to 0, 1, and 2 molecules inside the nanogap.[12]

measurement with 120 pM ferrocene added, which corresponds to 0.4 molecule on average being present in the nanogap based on its volume and nominal solution concentration (this is only an estimate due to adsorption of the redox species during sample preparation and inside the nanogap). Here the baseline becomes more noisy, and large excursions away from the baseline are observed on the scale of seconds. Importantly, these excursions have opposite polarities at the reducing and oxidizing electrodes and reverse when the potentials on the electrodes are swapped, consistent with redox cycling.[12] The longest events also exhibit plateau-like shapes with a step height of 20 fA (Figure 3c), and we attribute these plateau-like events to individual molecules entering the nanogap, undergoing redox cycling for a few seconds, and exiting the nanogap again. Importantly, the plateau height is ~4 times smaller than expected based on the assumption of ideal diffusive mass transport (eq 3). This level of suppression is consistent with the amount of adsorption typical of our nanogap devices[31,42,48] but represents a significant difference from earlier reports,[10,11] where eq 3 was assumed to hold.

Because of the low value of $i_0 = 20$ fA, the signal-to-noise ratio for long single-molecule events in Figure 3 is close to unity. Fortunately, it is nonetheless possible to extract quantitative evidence for single-molecule sensitivity from these data. To do so, note that each of the two simultaneously acquired amperometric traces consists of two components: the redox cycling current, which has the same magnitude but opposite signs at the two electrodes, and instrumental noise, which is independent for the two electrodes. This allows performance of a cross-correlation analysis to extract the amplitude of the faradaic fluctuations.[12] Importantly, this procedure is independent of subjective judgments and can be applied systematically to complete data sets rather than relying on the experimenter's judgment. The amplitude

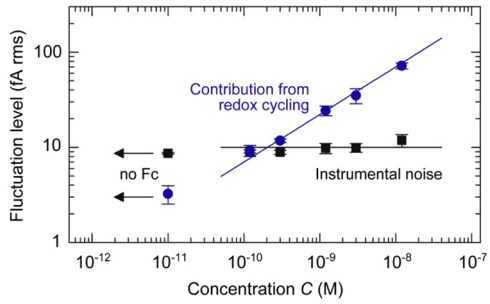

FIGURE 4. Cross-correlation analysis of amperometric data. Noise from the instrumentation is independent of the concentration of redox species (black line), while the faradaic contribution scales as $C^{1/2}$ (blue line).[12]

of the redox cycling fluctuations is predicted to scale as $C^{1/2}$, while the background noise should be independent of the concentration of the redox species. The experiments agree well with these predictions, as shown in Figure 4, providing independent, quantitative evidence that single-molecule resolution has been achieved.[12]

The next step is to compare the distribution of observed currents with the Poisson distribution. Ideally one would expect the current to be distributed among a finite number of discrete values $I(t) = Ni_0$ corresponding to $N = 0, 1, 2, ...$, the fraction of the time spent at each value of I being described by eq 1.[30] Histograms of current traces (as per Figure 3) however do not yield well-defined peaks, instead exhibiting a broad, smeared out distribution.[12] This lack of well-defined plateau values was initially quite troubling to us, because our estimates based on eqs 1 and 2 indicated that they should be discernible. Only a more detailed analysis of the complete signal transduction chain revealed the origin of this apparent discrepancy.[12]

In short, measurement electronics do not respond instantaneously: even if the real faradaic current $I(t)$ exhibits a sharp step, the current reported by the measurement

electronics, $I_{meas}(t)$, responds more gradually. Specifically, $I_{meas}(t)$ is given by the convolution of $I(t)$ with the so-called impulse response of the measurement system; in the simplest (first-order) approximation, this takes the form

$$I_{meas}(t) = \frac{1}{\tau}\int_0^\infty dt'\, e^{-t'/\tau} I(t - t') \qquad (4)$$

where τ is the rise time characterizing the measurement system. Qualitatively, the effect of eq 4 is to smooth out features in $I(t)$ that vary faster than τ. While such smoothing is unavoidable, it is particularly relevant here due to two coinciding factors. Because of the low (fA) current levels involved in our experiments, a high degree of amplification is required, and higher amplification necessarily implies slower electronics (via the so-called gain-bandwidth product). This leads to large values of τ in eq 4 and therefore to more smearing of $I(t)$. While not an issue if τ remained shorter than the duration of the features of interest, there is in fact no such well-defined "characteristic time" describing the dwell time of a molecule inside the nanogap: instead, the probability distribution for the events' duration diverges as $t^{-3/2}$ at short times.[12] This signifies that the vast majority of events are shorter than τ and therefore get smoothed out by the measurement.

Armed with this insight, it is straightforward to reproduce the features of the data using simple simulations of Brownian motion.[12] The simulated $N(t)$ is transformed into a current $I(t)$ using eq 2, the time response is accounted for using eq 4, and random noise is added based on the (quantifiable) properties of the electronics to yield $I_{meas}(t)$. The result is illustrated in Figure 5a, which clearly illustrates how the finite response time obscures a significant amount of the information present in the original $N(t)$ trace. In particular, short events do not allow the current to reach the full plateau value i_0, while many short events clustered together can give rise to spurious plateaus at current values between 0 and i_0; only the rare, long events actually yield well-defined plateaus. This explains why the "baseline" in Figure 3b appears noisier than that in Figure 3a: it in fact includes many short events that were too short to be resolved by our electronics. Unfortunately, we are not aware of a procedure to perform the reverse analysis, namely, to extract $P(N)$ from $I_{meas}(t)$ in the presence of additive noise. While mathematically rigorous algorithms exist for identifying steps in noisy data,[49] they cannot yet compensate for the finite time resolution described by eq 4.

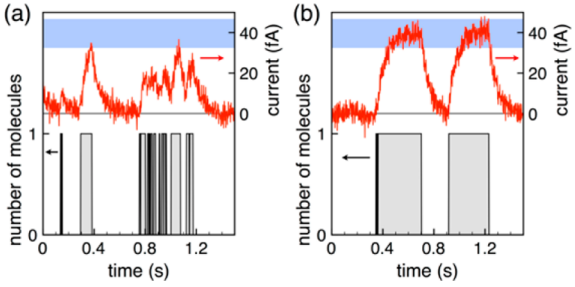

FIGURE 5. Random-walk simulations illustrating the effect of the response time of electronics on single-molecule amperometry. (a) Simulated molecule number $N(t)$ (black) and corresponding current $I_{meas}(t)$ (red) after accounting for the measurement electronics. The blue band indicates the steady-state single-molecule current, i_0; most events are too short to reach this level ($D = 5 \times 10^{-10}$ m^2 s^{-1}, nanogap length 100 μm, $\tau = 180$ ms, 3 fA$_{rms}$ added noise). (b) Corresponding data in the presence of advective flow (average velocity 250 μm s^{-1}). Single-molecule events now have a well-defined duration and reach the expected current level.

How can we overcome this limitation? One way is to prevent molecules from entering and leaving the nanogap by using valves to reversibly seal the measurement volume, in analogy with tip-based experiments[11] but with a high enough throughput that meaningful statistics can be accumulated. Alternatively, we can envision eliminating the very short events, which correspond to molecules entering the nanogap and immediately leaving again from the same side, using migrational or convective transport of the redox species through the nanogap. Rather than randomly entering and leaving, molecules would then be driven from one end of the nanogap device to the other, leading to single molecule events with a well-defined duration (apart from a small random correction from Brownian motion). The validity of this concept is corroborated by simulations,[34] as illustrated in Figure 5b.

Conclusions and Outlook

We started this Account by summarizing the motivations for striving to achieve single-molecule resolution in electrochemical measurements. How far along has our community come toward these goals?

We believe that significant advances have taken place toward better understanding the subtleties of single-molecule measurements and how to make connections with conventional electrochemistry. For instance, consequences of the high surface-to-volume ratio inherent to nanogap devices[50] have been elucidated, including double-layer-reorganization effects when the nanogap is sealed[11] and reversible adsorption of redox molecules,[31,42,48] which can drastically reduce the amperometric signature from

individual molecules. Both effects were largely neglected in early thinking on single-molecule electrochemistry.

The stochastic nature of single-molecule signals was also highlighted.[29,30] In particular, we argued above that it is insufficient to think solely in terms of the Poisson distribution (eq 1) to explain experimental single-molecule signals because these are strongly affected by the inevitable limit in time resolution of electrochemical instrumentation. On the other hand, Figures 3 and 4 show that it is possible to detect the signature of ~100 pM redox species by looking at current fluctuations. This would be nearly impossible using conventional measurements such as steady-state voltammetry, highlighting the potential benefits of developing new analysis techniques for treating electrochemical data at the nanoscale.

What about the broader aims of developing single-molecule electrochemical techniques and creating a new experimental platform that can be employed to study (bio)catalytic systems or serve as a basis for new analytical capabilities? Clearly, this has not yet been achieved: single-molecule electrochemistry experiments so far have mostly focused on the more modest aim of proving that single-molecule resolution is at all possible. That said, we are optimistic that this situation will change in the near future. Now that single-molecule detection has been demonstrated in microfabricated devices, at least at the proof-of-concept level, the versatility and flexibility of the approach should allow introduction of a series of stepwise refinements that can collectively lead to major performance improvements. These include optimizing device geometry so that nanogaps with $z \approx 10$ nm can be reproducibly and verifiably produced, minimizing adsorption through the flexible choice of materials, and suppressing diffusion noise by advecting samples through the detection volume, as illustrated in Figure 5b, or by integrating microfluidic valves allowing "closed volume" measurements with rapid throughput. Importantly, each of these improvements can be achieved via iterative design without reinventing the basic approach.

Our opinion that microfabricated systems are the most promising route to reliable single-molecule electrochemistry is of course based on present knowledge and could be overturned by unforeseen game-changing insights and experiments. But such developments would only serve to accelerate the adoption of single-molecule electrochemistry as a routinely applicable technique, which can open the door to a fascinating array of fundamental experiments and analysis methods.

We wish to thank all colleagues, past and present, who have participated in our work on single-molecule electrochemistry and, in particular, M. A. G. Zevenbergen, E. D. Goluch, B. Wolfrum, and E. Kätelhön. We gratefully acknowledge financial support from NanoNed, the Netherlands Organization for Scientific Research (NWO), and the European Research Council (ERC).

BIOGRAPHICAL INFORMATION

Serge G. Lemay was born in Rimouski, Canada, in 1970. He received a B.A.Sc. in Electrical Engineering with minor in Physics from the University of Waterloo, Canada, in 1993, and a Ph.D. in Physics from Cornell University, Ithaca, NY, USA, in 1999. He was faculty at the Kavli Institute of Nanoscience, Delft University of Technology, The Netherlands, from 2001 to 2009. In 2009, he founded the Nanoionics group at the MESA+ Institute for Nanotechnology, University of Twente, The Netherlands. His main research interests at present include electrostatics in liquids, the fundamentals of electroosmosis, and electrochemical nanofluidics.

Shuo Kang was born in Changchun, China, in 1983. She received her B.Sc. in Electrical Engineering from Jilin University, China, in 2004, and a M.Sc. in Microelectronics from Delft University of Technology, The Netherlands, in 2006. She was a MEMS product engineer at Concept to Volume, The Netherlands, from 2006 to 2010. She is currently a Ph.D. candidate in the Nanoionics group at the MESA+ Institute for Nanotechnology working on single-molecule detection in electrochemical nanofluidic devices.

Klaus Mathwig was born in Berlin, Germany, in 1980. He studied Nanostructuring Technology at the Julius-Maximilians-Universität Würzburg, Germany, and received his Ph.D. from the Max Planck Institute of Microstructure Physics in Halle, Germany, in 2010. He was a postdoctoral associate at the ETH Zürich, Switzerland, before joining the Nanoionics group at the University of Twente in 2011. His research interests include electrochemical nanofluidics, Brownian ratchets, and impedance spectroscopy.

Pradyumna S. Singh was born in Baroda, India, in 1978. He received his B.Sc. in Chemistry from The Maharaja Sayajirao University, India, and his Ph.D. from the University of Arizona, Tucson, AZ, USA, in 2005 under the direction of D. H. Evans. After a postdoctoral stay with Leif Hammarström at Uppsala University, Sweden, he joined Serge Lemay's laboratory at the Kavli Institute for Nanoscience at Delft in 2008. His research interests include mesoscopic and single-molecule electrochemistry and using nanofabricated electrochemical devices for sensitive biosensing applications.

FOOTNOTES

*Corresponding author. E-mail: s.g.lemay@utwente.nl.
The authors declare no competing financial interest.

REFERENCES

1 Maxwell, J. C. *Theory of Heat*; Longman, Green and Co: London, 1871.
2 Walter, N. G.; Huang, C.-Y.; Manzo, A. J.; Sobhy, M. A. Do-it-yourself guide: How to use the modern single-molecule toolkit. *Nat. Methods* **2008**, *5*, 475–489.

3 *Handbook of Single-Molecule Biophysics*; Hinterdorfer, P., van Oijen, A., Eds.; Springer: Dordrecht, the Netherlands, 2009.

4 Moerner, W. E.; Wild, U. P.; Basche, T. *Single-Molecule Optical Detection, Imaging and Spectroscopy*; VCH Verlagsgesellschaft mbH: Weinheim, Germany, 2008.

5 Neuman, K. C.; Nagy, A. Single-molecule force spectroscopy: Optical tweezers, magnetic tweezers and atomic force microscopy. *Nat. Methods* **2008**, *5*, 491–505.

6 Zhang, J.; Kuznetsov, A. M.; Medvedev, I. G.; Chi, Q.; Albrecht, T.; Jensen, P. S.; Ulstrup, J. Single-Molecule Electron Transfer in Electrochemical Environments. *Chem. Rev.* **2008**, *108*, 2737–2791.

7 Liphardt, J.; Dumont, S.; Smith, S. B.; Tinoco, I.; Bustamante, C. Equilibrium information from nonequilibrium measurements in an experimental test of Jarzynski's equality. *Science* **2002**, *296*, 1832–1835.

8 Hilario, J.; Kowalczykowski, S. C. Visualizing protein-DNA interactions at the single-molecule level. *Curr. Opin. Chem. Biol.* **2010**, *14*, 15–22.

9 Bustamante, C.; Macosko, J. C.; Wuite, G. J. L. Grabbing the cat by the tail: Manipulating molecules one by one. *Nat. Rev. Mol. Cell Biol.* **2000**, *1*, 130–136.

10 Fan, F. R. F.; Bard, A. J. Electrochemical detection of single molecules. *Science* **1995**, *267*, 871–874.

11 Sun, P.; Mirkin, M. V. Electrochemistry of individual molecules in zeptoliter volumes. *J. Am. Chem. Soc.* **2008**, *130*, 8241–8250.

12 Zevenbergen, M. A. G.; Singh, P. S.; Goluch, E. D.; Wolfrum, B. L.; Lemay, S. G. Stochastic sensing of single molecules in a nanofluidic electrochemical device. *Nano Lett.* **2011**, *11*, 2881–2886.

13 Palacios, R. E.; Fan, F.-R. F.; Bard, A. J.; Barbara, P. F. Single-molecule spectroelectrochemistry (SMS-EC). *J. Am. Chem. Soc.* **2006**, *128*, 9028–9029.

14 Lei, C.; Hu, D.; Ackerman, E. Clay nanoparticle-supported single-molecule fluorescence spectroelectrochemistry. *Nano Lett.* **2009**, *9*, 655–658.

15 Lei, C.; Hu, D.; Ackerman, E. J. Single-molecule fluorescence spectroelectrochemistry of cresyl violet. *Chem. Commun.* **2008**, 5490–5492.

16 Cortés, E.; Etchegoin, P. G.; Le Ru, E. C.; Fainstein, A.; Vela, M. E.; Salvarezza, R. C. Monitoring the electrochemistry of single molecules by surface-enhanced Raman spectroscopy. *J. Am. Chem. Soc.* **2010**, *132*, 18034–18037.

17 Branton, D.; Deamer, D. W.; Marziali, A.; Bayley, H.; Benner, S. A.; Butler, T.; Di Ventra, M.; Garaj, S.; Hibbs, A.; Huang, X.; Jovanovich, S. B.; Krstic, P. S.; Lindsay, S.; Ling, X. S.; Mastrangelo, C. H.; Meller, A.; Oliver, J. S.; Pershin, Y. V.; Ramsey, J. M.; Riehn, R.; Soni, G. V.; Tabard-Cossa, V.; Wanunu, M.; Wiggin, M.; Schloss, J. A. The potential and challenges of nanopore sequencing. *Nat. Biotechnol.* **2008**, *26*, 1146–1153.

18 Dekker, C. Solid-state nanopores. *Nat. Nanotechnol.* **2007**, *2*, 209–215.

19 Kasianowicz, J. J.; Robertson, J. W. F.; Chan, E. R.; Reiner, J. E.; Stanford, V. M. Nanoscopic porous sensors. *Annu. Rev. Anal. Chem.* **2008**, *1*, 737–766.

20 Lathrop, D. K.; Ervin, E. N.; Barrall, G. A.; Keehan, M. G.; Kawano, R.; Krupka, M. A.; White, H. S.; Hibbs, A. H. Monitoring the escape of DNA from a nanopore using an alternating current signal. *J. Am. Chem. Soc.* **2010**, *132*, 1878–1885.

21 Zhang, J.; Chi, Q.; Albrecht, T.; Kuznetsov, A. M.; Grubb, M.; Hansen, A. G.; Wackerbarth, H.; Welinder, A. C.; Ulstrup, J. Electrochemistry and bioelectrochemistry towards the single-molecule level: Theoretical notions and systems. *Electrochim. Acta* **2005**, *50*, 3143–3159.

22 Li, T.; Hu, W.; Zhu, D. Nanogap electrodes. *Adv. Mater.* **2010**, *22*, 286–300.

23 Nichols, R. J.; Haiss, W.; Higgins, S. J.; Leary, E.; Martin, S.; Bethell, D. The experimental determination of the conductance of single molecules. *Phys. Chem. Chem. Phys.* **2010**, *12*, 2801–2815.

24 Selzer, Y.; Allara, D. L. Single-molecule electrical junctions. *Annu. Rev. Phys. Chem.* **2006**, *57*, 593–623.

25 Xiao, X.; Bard, A. J. Observing single nanoparticle collisions at an ultramicroelectrode by electrocatalytic amplification. *J. Am. Chem. Soc.* **2007**, *129*, 9610–9612.

26 Anderson, L. B.; Reilley, C. N. Thin-layer electrochemistry: Use of twin working electrodes for the study of chemical kinetics. *J. Electroanal. Chem.* **1965**, *10*, 538–52.

27 Anderson, L. B.; Reilley, C. N. Thin-layer electrochemistry: Steady-state methods of studying rate processes. *J. Electroanal. Chem.* **1965**, *10*, 295–305.

28 Cutress, I. J.; Dickinson, E. J. F.; Compton, R. G. Electrochemical random-walk theory Probing voltammetry with small numbers of molecules: Stochastic versus statistical (Fickian) diffusion. *J. Electroanal. Chem.* **2011**, *655*, 1–8.

29 Kätelhön, E.; Wolfrum, B. Simulation-based investigations on noise characteristics of redox-cycling sensors. *Phys. Status Solidi A* **2012**, *209*, 881–884.

30 Bard, A. J.; Fan, F. R. F. Electrochemical detection of single molecules. *Acc. Chem. Res.* **1996**, *29*, 572–578.

31 Zevenbergen, M. A. G.; Singh, P. S.; Goluch, E. D.; Wolfrum, B. L.; Lemay, S. G. Electrochemical correlation spectroscopy in nanofluidic cavities. *Anal. Chem.* **2009**, *81*, 8203–8212.

32 Fan, F. R. F.; Kwak, J.; Bard, A. J. Single molecule electrochemistry. *J. Am. Chem. Soc.* **1996**, *118*, 9669–9675.

33 Mathwig, K.; Mampallil, D.; Kang, S.; Lemay, S. G. Electrical cross-correlation spectroscopy: Measuring picoliter-per-minute flows in nanochannels. *Phys. Rev. Lett.* **2012**, *109*, No. 118302.

34 Singh, P. S.; Kätelhön, E.; Mathwig, K.; Wolfrum, B.; Lemay, S. G. Stochasticity in single-molecule nanoelectrochemistry: origins, consequences and solutions. *ACS Nano* **2012**, *6*, 9662–9671.

35 Zevenbergen, M. A. G.; Wolfrum, B. L.; Goluch, E. D.; Singh, P. S.; Lemay, S. G. Fast electron-transfer kinetics probed in nanofluidic channels. *J. Am. Chem. Soc.* **2009**, *131*, 11471–11477.

36 Feldberg, S. W. Implications of Marcus−Hush theory for steady-state heterogeneous electron transfer at an inlaid disk electrode. *Anal. Chem.* **2010**, *82*, 5176–5183.

37 Amatore, C.; Fosset, B.; Bartelt, J.; Deakin, M. R.; Wightman, R. M. Electrochemical kinetics at microelectrodes: Part V. Migrational effects on steady or quasi-steady-state voltammograms. *J. Electroanal. Chem. Interfacial Electrochem.* **1988**, *256*, 255–268.

38 Elsamadisi, P.; Wang, Y.; Velmurugan, J.; Mirkin, M. V. Polished nanopipets: New probes for high-resolution scanning electrochemical microscopy. *Anal. Chem.* **2011**, *83*, 671–673.

39 Cox, J. T.; Zhang, B. Nanoelectrodes: Recent Advances and New Directions. *Annu. Rev. Anal. Chem.* **2012**, *5*, 253–272.

40 Singh, P. S.; Goluch, E. D.; Heering, H. A.; Lemay, S. G. Nanoelectrochemistry: Fundamentals and Applications in Biology and Medicine. In *Applications of Electrochemistry and Nanotechnology in Biology and Medicine II*; Eliaz, N., Ed.; Springer: New York, 2012; Vol. 53, pp 1−66.

41 Rothberg, J. M.; Hinz, W.; Rearick, T. M.; Schultz, J.; Mileski, W.; Davey, M.; Leamon, J. H.; Johnson, K.; Milgrew, M. J.; Edwards, M.; Hoon, J.; Simons, J. F.; Marran, D.; Myers, J. W.; Davidson, J. F.; Branting, A.; Nobile, J. R.; Puc, B. P.; Light, D.; Clark, T. A.; Huber, M.; Branciforte, J. T.; Stoner, I. B.; Cawley, S. E.; Lyons, M.; Fu, Y.; Homer, N.; Sedova, M.; Miao, X.; Reed, B.; Sabina, J.; Feierstein, E.; Schorn, M.; Alanjary, M.; Dimalanta, E.; Dressman, D.; Kasinskas, R.; Sokolsky, T.; Fidanza, J. A.; Namsaraev, E.; McKernan, K. J.; Williams, A.; Roth, G. T.; Bustillo, J. An integrated semiconductor device enabling non-optical genome sequencing. *Nature* **2011**, *475*, 348–352.

42 Kang, S.; Mathwig, K.; Lemay, S. G. Response time of nanofluidic electrochemical sensors. *Lab Chip* **2012**, *12*, 1262–1267.

43 Kätelhön, E.; Hofmann, B.; Lemay, S. G.; Zevenbergen, M. A. G.; Offenhausser, A.; Wolfrum, B. Nanocavity redox cycling sensors for the detection of dopamine fluctuations in microfluidic gradients. *Anal. Chem.* **2010**, *82*, 8502–8509.

44 Rassaei, L.; Singh, P. S.; Lemay, S. G. Lithography-Based Nanoelectrochemistry. *Anal. Chem.* **2011**, *83*, 3974–3980.

45 Kätelhön, E.; Wolfrum, B. On-chip redox cycling techniques for electrochemical detection. *Rev. Anal. Chem* **2012**, *31*, 7–14.

46 Zevenbergen, M. A. G.; Krapf, D.; Zuiddam, M. R.; Lemay, S. G. Mesoscopic concentration fluctuations in a fluidic nanocavity detected by redox cycling. *Nano Lett.* **2007**, *7*, 384–388.

47 Hofmann, B.; Kaetelhoen, E.; Schottdorf, M.; Offenhaeusser, A.; Wolfrum, B. Nanocavity electrode array for recording from electrogenic cells. *Lab Chip* **2011**, *11*, 1054–1058.

48 Singh, P. S.; Chan, H. S. M.; Kang, S.; Lemay, S. G. Stochastic amperometric fluctuations as a probe for dynamic adsorption in nanofluidic electrochemical systems. *J. Am. Chem. Soc.* **2011**, *133*, 18289–18295.

49 Bozorgui, B.; Shundyak, K.; Cox, S. J.; Frenkel, D. Free-energy-based method for step size detection of processive molecular motors. *Eur. Phys. J. E* **2010**, *31*, 411–417.

50 Bocquet, L.; Charlaix, E. Nanofluidics, from bulk to interfaces. *Chem. Soc. Rev.* **2010**, *39*, 1073–1095.